EDUCTION OF TURBULENT STRUCTURES IN A THERMAL BOUNDARY LAYER FLOW

Gaetano Iuso, Michele Onorato
Dipartimento di Ingegneria Aerospaziale, Politecnico di Torino, Italy

Miguel Onorato
Dipartimento di Fisica Generale, Università di Torino, Italy

Abstract

Measurements of velocity and temperature in a thermal boundary layer flow are shown and results are compared with published data.

An eduction method of characteristic turbulent events, intermittent production of fluctuating turbulent energy, based on wavelet transform, is presented. The method is applied to measurements in the near wall turbulent boundary layer, $y^+=15$, in order to evaluate the distribution of the number of events per unit time among time scales and in order to obtain the spectral contribution of these events to the mean energy spectrum. Dominant frequencies and scales for the turbulent events are determined for the velocity and for the temperature signals.

The velocity and the temperature fields, even though if measurements were taken independently, give very similar results, at least for wall temperature slightly different from the temperature of the external flow.

Introduction

It is well known that *bursting* processes, intermittent motions of intense turbulence activity, play an important role in maintaining the turbulence production mechanism in the inner layer and are responsible of most of the turbulent transport phenomena near the wall.

A detailed understanding of these motions (events) is of great interest both for modelling the dynamics of the flow and for developing methods to control skin friction, wall heat transfer and aerodynamic noise.

A great amount of work has been produced on the subject, since the pioneering papers of Kline et al.[1] and Corino et al. [2]. A comprehensive review is given in papers of Hussain [3] and Robinson [4].

The studies on the subject rely heavily on flow visualisation and hot wire measurements (Refs. 5-13) and more recently on direct numerical simulation (DNS) of boundary layer and fully developed channel flows (Refs. 14-18). It has become increasingly clear, especially after the DNS results, that bursting motions are linked to the dynamics of organised coherent vortical structures in the wall region. These structures appear in a variety of repetitive forms and at different scales and levels of activity.

In spite of the considerable amount of information obtainable by the direct numerical simulation, the experimental approach is still of great importance, being the DNS restricted to simple flow configurations and to very low Reynolds numbers, far from most of the practical applications. Moreover, the three dimensional nature of the motions of interest and the facts that events are embedded inside the overall random behaviour of the turbulence field, make their eduction a very complex task, especially for single-point Eulerian measurements.

Several techniques for detecting bursting events have been developed during the past twenty years. These techniques are based on the local variance of the streamwise u-velocity component (VITA[6,7]), on the mean local gradient of the signal (WAG[19]), on the local value of the u-velocity (u-level[5]), or on its slope[20] and on the sign of the uv product (Quadrant method[9]). All these detection algorithms rely on the assumption of a threshold, whose value is empirically established, mostly by correlation with flow visualisation results.

In this paper, a detection method, based on wavelet spectral analysis, is applied to study bursting motions in a thermal boundary layer flow in a nominally zero pressure gradient. Results from VITA detection scheme are also included in the paper as a reference to published work on the same subject.

Kim and Moin[21], performing direct numerical simulation of a turbulent channel flow with passive scalars, found that the temperature field are highly correlated with the streamwise velocity; the correlation coefficient between the temperature and the velocity was as high as 0.95. In Refs 22-25, the temperature has been used as a passive contaminant to mark the flow in order to provide plausible links between the bursting phenomenon and the large wall structure.

Copyright © 1996 by the AIAA and ICAS. All rights reserved.

It is part of the present research to consider different wall temperature conditions; only results for the case of wall temperature slightly different from the external flow temperature are shown in this paper.

Experimental apparatus

The experiments were conducted on a splitter plate, mounted horizontally in the test section of the 0.70 m x 0.50 m, low speed, open circuit wind tunnel of the "Modesto Panetti" laboratory of the "Politecnico di Torino". The pressure gradient along the plate was nearly zero. The plexiglas plate covered by a polyurethane foam, spans the 0.70 m of the test section and extends from 0.2 m downstream of the test section entrance to a total length of 3.5 m. The transition to turbulent flow is artificially fixed at the plate leading edge. The plate is covered by a very thin printed circuit board which is glued over the polyurethane foam (20 mm thick); the circuit is used to generate, by Joule effect, a uniform heat flux distribution on the surface, allowing a temperature difference between the flat plate surface and the air stream. The wall temperature is measured by an infrared thermograph (spot 8 mm, error = ± 1%). Single normal hot wire probes have been used for turbulence measurements. A Dantec type 55P11 probe, 1. mm long, with a diameter of 5 μm, was used for the longitudinal velocity fluctuations, and a Dantec type 55P31, of length 0.25 mm, diameter 1μm, was used for temperature fluctuation measurements. The a.c. part of the probe signals, amplified by 10, was acquired by a 12 bit analog-to-digital converter at 18 KHz sampling rate for velocity measurements and 6 KHz for temperature. The accuracy may be evaluated within 2% for both measurements. The hot wires were calibrated in velocity and temperature. The distance of the probes from the splitter plate was measured within 0.01 mm.

VITA detection scheme

The VITA technique[6], permits a local measure of the turbulent activity and is based on the intermittent character of the short-time variance of a turbulent velocity signal. The short-time variance of a fluctuating velocity component $u(t)$ is defined as follows:

$$\mathrm{var}_u(\tau,T)=\frac{1}{T}\int_{\tau-T/2}^{\tau+T/2}[u(t)]^2\,dt-\left[\frac{1}{T}\int_{\tau-T/2}^{\tau+T/2}[u(t)]dt\right]^2, \quad (1)$$

where T is the window in which the short-time variance is calculated. An event is considered to occur when $\mathrm{var}_u(\tau,T)$ exceeds the quantity ku_{rms}^2, where k is a chosen threshold level and u_{rms}^2 is the total variance of the signal. Detected events are classified as *accelerating* motions if $\partial u/\partial t>0$ and *decelerating* motions if $\partial u/\partial t<0$ (see Ref. 26).

In this technique, a detection corresponds to a continuous portion of the signal where the threshold conditions are satisfied. The detection time, τ_j, is defined as the mid point of the event duration. Once the reference times are determined, a conditional average of signal $s(t)$ can be calculated as follows:

$$<s(\tau')>=\frac{1}{N}\sum_{j=1}^{N}s(\tau_j+\tau'), \quad (2)$$

where N is the number of events and τ' is a time relative to the reference time τ_j.

The VITA scheme is strongly dependent on the value of the threshold constant, k, and on the value of the averaging time window, T, which acts as a filter on the signal. In Ref. 27 it is shown that the number of events detected decrease exponentially with increasing threshold level k and the band-pass filter character of the short-time window T is demonstrated.

In this paper, accepted values for T and k are adopted as they were selected in many investigations by correlation with flow visualisations or multi-point measurements.

Fundamentals on Wavelet Analysis

Wavelet transform has been widely used for analysing different turbulent fields (see Farge's paper[28] for comments and references). Application of wavelet analysis to boundary layer have been performed by Liandrat et al. [29] and by Benaissa et al. [24].

To establish notations, the basic formulas that will be used in the analysis of the data are shown. Mathematical details can be found in Refs. 28,30,31.

A wavelet is any square integrable, real or complex valued function $\psi(t)$ that satisfies the *admissibility condition*:

$$C_\psi=\int_{-\infty}^{\infty}\left|\hat{\psi}(\omega)\right|^2|\omega|^{-1}d\omega<\infty, \quad (3)$$

where $\hat{\psi}(\omega)$ is the Fourier transform of $\psi(t)$. Condition (3) implies that $\psi(t)$ has a zero mean value. The wavelet transform of a function $s(t)$ consists of all correlation of $s(t)$ with an infinite family of functions obtained from $\psi(t)$ by continuous dilation and translation. More precisely, the family of functions is defined as follows:

$$\psi_{a\tau}=a^{-1/2}\psi\left(\frac{t-\tau}{a}\right), \quad (4)$$

where a is the scale parameter, also known as wavelet scale, and τ is the translation parameter; the factor $a^{-1/2}$ allows the L^2-norm of $\psi_{a\tau}$ to be independent of a. The continuous wavelet transform of a function $s(t)$ is given by:

$$W(a,\tau) = \int_{-\infty}^{\infty} s(t)\,\psi^*_{a\tau}\,dt, \qquad (5)$$

Using the theorem of convolution, it can be shown that the wavelet coefficients can also be calculated in the following way:

$$W(a,\tau) = (1/2\pi)a^{1/2}\int_{-\infty}^{\infty} \hat{f}(\omega)[\hat{\psi}(a\omega)]^* e^{i\omega\tau}d\omega \qquad (6)$$

Thus, $W(a,\tau)$, at each scale a, can be interpreted as a filtered version of $s(t)$, where the filters are given by the Fourier transform of the wavelets at each scale.

For the continuous wavelet transform, the wavelets are not orthogonal and the coefficients contains redundant information; nevertheless, if the admissibility condition (3) is satisfied, the corresponding inverse wavelet transform can be written:

$$s(t) = \left(1/C_\psi\right)\int_{-\infty}^{\infty}\int_{0}^{\infty} W(a,\tau)\psi^*_{a\tau}\,d\tau da \;/\; a^2. \qquad (7)$$

Just like in the Fourier transform, the Parseval's theorem holds:

$$\int_{-\infty}^{\infty}|s(t)|^2\,dt = \left(1/C_\psi\right)\int_{-\infty}^{\infty}\int_{0}^{\infty}|W(a,\tau)|^2\,d\tau da \;/\; a^2. \qquad (8)$$

Therefore, the wavelet transform preserves energy not only globally but also locally; the integrand function at the right hand side, which is an energy per unit of time and frequency, may be used to detect instants of time and scales that contribute mostly to the energy. In the past literature, the spectral content of a signal has being given, using the Fourier transform, in terms of an energy as a function of frequency. In order to compare wavelet and Fourier results, it is useful to define the *wavelet frequency*, $f = c/(2\pi a)$, that plays the same role as the frequency in the Fourier analysis; c is a constant and depends on the family of wavelet used. For visualisation purposes, f is usually sampled logarithmically, thus equation (8) formally can be expressed as follows:

$$\int_{-\infty}^{\infty}|s(t)|^2\,dt = \left(1/C_\psi\right)(2\pi/c)\int_{-\infty}^{\infty}\int_{-\infty}^{\infty}|W(f,\tau)|^2\,f\,d\tau d\ln f \qquad (9)$$

Integration in τ of $|W(f,\tau)|^2$ in the right hand side of equation (9) gives the *wavelet power spectrum,*

$$P(f) = \left(1/C_\psi\right)\int_{-\infty}^{\infty}|W(f,\tau)|^2\,d\tau \qquad (10)$$

which, as shown by Hudgins et al. [32], is a smoother and clearer representation than the one obtained with the classical Fourier analysis. Moreover, by integrating in frequency $|W(f,\tau)|^2$, the *wavelet local energy* is obtained:

$$E(\tau) = \int_{-\infty}^{\infty}|W(f,\tau)|^2\,f\,d\ln f. \qquad (11)$$

As it will be shown, the function $E(\tau)$ will be used to detect instants of time at which events occur.

Basic flow results

The data here analysed are taken at a Reynolds number, based on momentum thickness, ϑ, and on the external velocity, of 1130. The temperature difference, $\Delta\theta$, between the wall and the external flow is 11.6° C. Other flow parameters at the measurement station x are: $Re_x = 8.8\,10^5$, $H = \delta^*/\vartheta = 1.34$ and $H_\theta = \delta^*_\theta/\vartheta_\theta = 1.47$. Independent measurements of the longitudinal component of the velocity and of the temperature were performed at different heights from the wall. The distribution across the boundary layer of mean velocity and temperature, U^+ and Θ^+, in comparison with the kinematic and the thermal law of the wall, are shown in figure 1; y^+ represents the distance from the wall. All quantities with superscript '+' are normalised respect to the viscous wall length, ν/u_τ and viscous time ν/u_τ^2, where u_τ is the skin friction velocity. A much better agreement between the temperature distribution and the thermal law of the wall has been found at higher Reynolds numbers, not shown here.

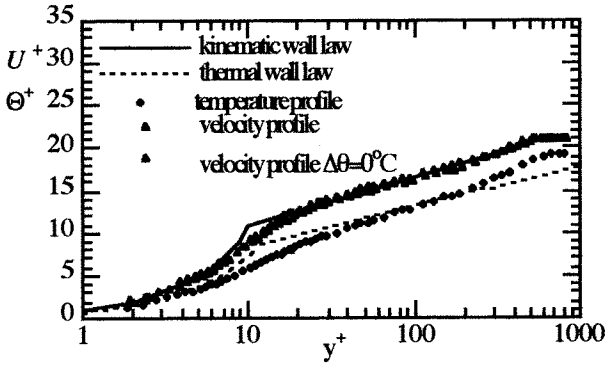

FIGURE 1 - Velocity and temperature profiles in comparison with the law of the wall

In figures 2 and 3, profiles of the root mean square value of velocity and temperature fluctuations are displayed. Skewness and flatness are shown in figures 4-7.

There is a reasonably good agreement between the present results and the data from other investigations[33,20], also included in the figures for comparison.

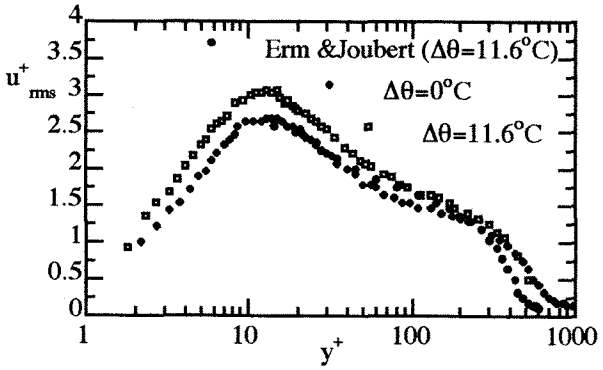

FIGURE 2 - Velocity fluctuations across the boundary layer

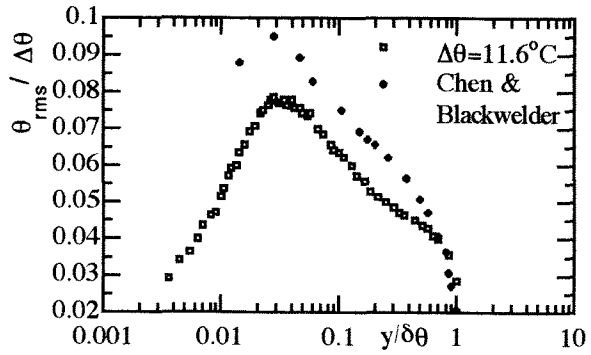

FIGURE 3 - Temperature fluctuations across the boundary layer

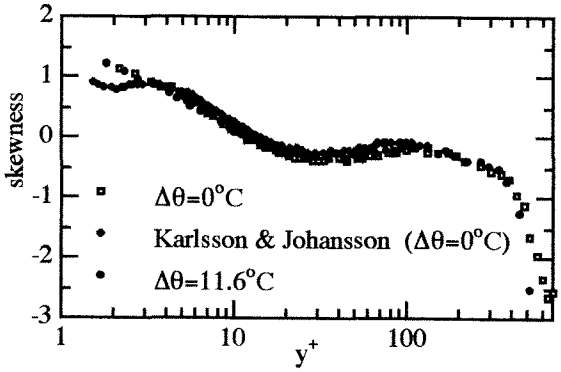

FIGURE 4 - Skewness for velocity across the boundary layer

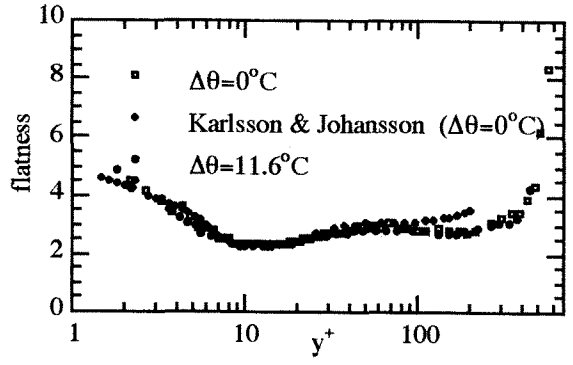

FIGURE 5 - Flatness for velocity across the boundary layer

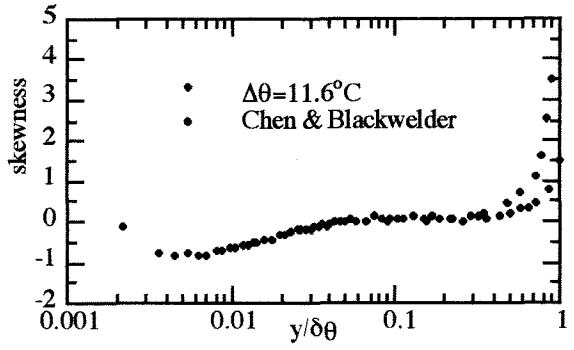

FIGURE 6 - Skewness for temperature across the boundary layer

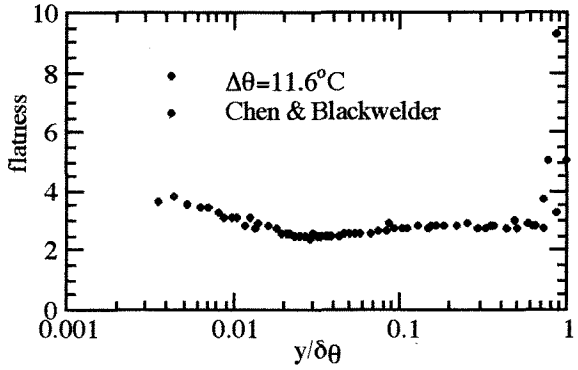

FIGURE 7 - Flatness for temperature across the boundary layer

Small differences may be attributed to peculiarities of small Reynolds number boundary layer flow of the present investigation. Reynolds number has been kept low in order to increase the wall viscous characteristics length, respect to probe dimension, l, and avoid spatial-averaging effects and assure consistent results for event eduction ($u_\tau l / \nu = 20$ for the velocity probe).

Event eduction results

A further comparison with published results[7] is shown in figure 8, where the number of VITA (k=1.2, T^+=10) accelerated events per unit of time, n^+_{VITA}, is reported as a function of the wall distance, for the velocity signal. It is confirmed that n^+_{VITA} is nearly constant in the wall region and it assumes a value not far from 0.005. The hot and cold cases give nearly the same results.

As already noted, the number of events per unit of time detected by VITA method varies strongly with the threshold k and the integration time T. It has been shown in Ref. 27 that n^+_{VITA} can be interpreted as a frequency of occurrence of events with time scales about 30% larger than T.

In order to give a contribution to the studies on the identification of characteristic turbulent events, the continuous wavelet decomposition analysis has been applied to the present data. Streamwise velocity component and temperature signals at $y^+ = 15$ are

considered.

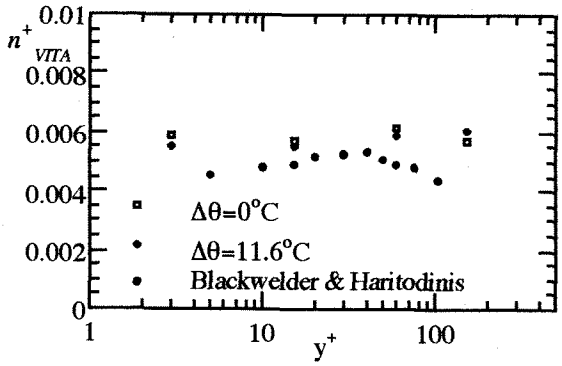

FIGURE 8 - Number of VITA events per unit of time across the boundary layer, for velocity signal

In figure 9, wavelet energy map, $|W(f,\tau)|^2 f$, is shown as a contour plot in the time-frequency plane. It is recalled that the frequency f is defined as $f = c/(2\pi a)$, where a is the wavelet scale parameter. For the present analysis the second derivative of the Gaussian function, also known as *Mexican hat* wavelet (see Ref. 35 for its properties), is used. For this wavelet, constant c is assumed to be equal to $2^{1/2}$. In figure 9, time t is normalized with the sampling interval Δt; ordering numbers N, in the frequency-axis, correspond to decreasing frequencies. The intermittent nature of the signal is evident from the plot, where intense turbulent activities (events, bursts) are shown to occur at different times. It is also evident the variety of scales involved in these intense turbulent activities. Peak values in the map are observed from N=8 to N=16, showing dominant frequencies of the velocity fluctuation intensity ranging from about 50Hz (N=16) Hz to 600Hz (N=8).

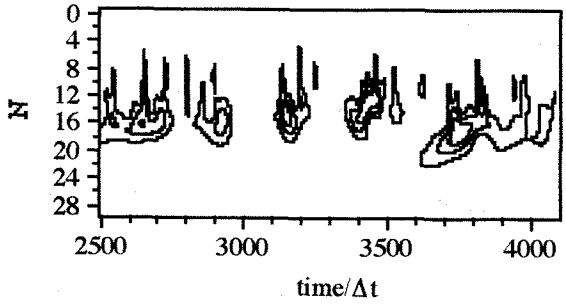

FIGURE 9 - Energy map for a portion of a velocity signal at $y^+ = 15$

Similar results are shown in figure 10 for the temperature, where peak values range from 20Hz (N=16) to 400Hz (N=6).

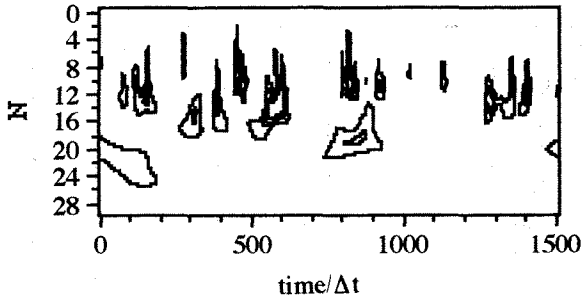

FIGURE 10 - Energy map for a portion of a temperature signal at $y^+ = 15$

The spectral-temporal resolution of the signal in the wavelet energy map, as in figures 9 and 10, are used for the eduction of individual events. Several algorithms of scanning for local maxima in the energy map can be performed (see, for instance, Higuchi et al.[36]). In our application, a simple scanning procedure has been applied. The function $E(\tau)$, defined in equation (11), is considered. A treshold is set in order to determine reference times τ_j at which the events ocurr. A function $D(\tau)$ is then constructed such that $D(\tau) = 0$ always, except for $\tau = \tau_j$. A second function, $DW(f,\tau)$, is then defined as follows:

$$DW(f,\tau) = 1 \quad \text{if} \quad \tau_j - \frac{1}{2}T_j \le \tau \le \tau_j + \frac{1}{2}T_j, \quad \forall f$$

$$DW(f,\tau) = 0 \qquad \text{else,} \qquad \forall f$$

where $T_j = 2\pi a_j / 2^{1/2}$, is the period of time duration corresponding to the frequency at which the maximum in $|W_u(f,\tau)|^2 f$ map at reference time τ_j, is found. $D(\tau)$ and $DW(f,\tau)$ may then be used as a mask for conditional, statistical and spectral analysis of the signal.

In figure 11, function $D(\tau)$ (fig. 11a), in comparison with events detected by VITA method (fig. 11b), is shown for a portion of the velocity signal corresponding to the map in figure 9. The correspondence is fairly good for the events that could be detected by VITA, assuming $T^+ = 10$. The thresholding criterion adopted for the results in figure 11 and for the analysis that will be shown in the following, consists simply on comparing the function $E(\tau)$ with k_W times its mean value, where k_W is a constant. In figure 11a, k_W is set equal to 2.1.

The dependence of number of events per unit of time, n^+_{to}, from the threshold constant k_W, is shown in figure 12 for the temperature and the velocity signals. In the figure, the events are classified in events with positive signal slope and events with negative signal slope. It can be seen that the velocity and temperature signals, that have been taken independently, give comparable values of n^+_{tot} for nearly the same value of the threshold k_W.

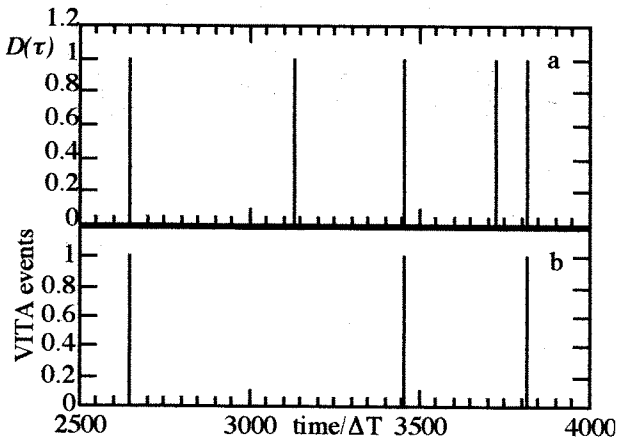

FIGURE 11 - Wavelet events, (a), and VITA events, (b), for a portion of a velocity signal at $y^+ = 15$

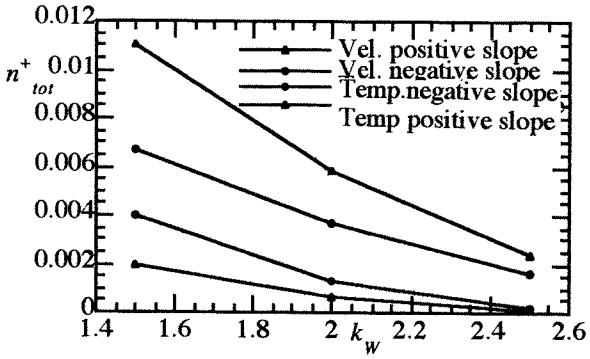

FIGURE 12 - Dependence of n^+_{tot} from the threshold constant

Two applications concerning with the distribution of occurrence of events per unit time among duration (scales) and with the conditional spectral analysis of the signals will be shown.

In figure 13, the number of events per unit time, is displayed as a function of the duration T for the velocity (k_W=2.1) and for the temperature (k_W=1.9) signals.

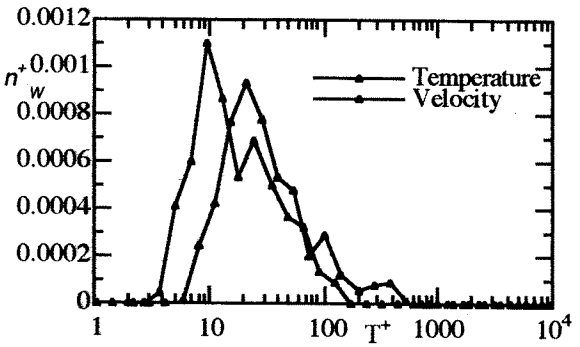

FIGURE 13 - Number of events per unit time in function of duration

For both cases the total number of events per unit time, in normalised form, is about 0.006. All events have been taken into account independently of the slope of the signal at the detection time. The duration value for which n_W^+ has its maximum corresponds to about 10-12 viscous time units for the velocity signal. The n_W^+ distribution for the temperature signal reaches its peak value at T^+= 20-22 viscous time units, showing that the probability for event occurrence at large duration is greater for the temperature field than for the velocity field. However, the results in figure 13 confirm that a large variety of scales are involved in the bursting motions, going from few viscous time units to more than 100 viscous time units.

A much larger range of scales are, involved in the spectral distributions of the signal energies. In figures 14 and 15 the wavelet mean (total) and conditional spectra, respectively for the velocity (k_W=2.1) and the temperature (k_W=1.9) signals, are shown.

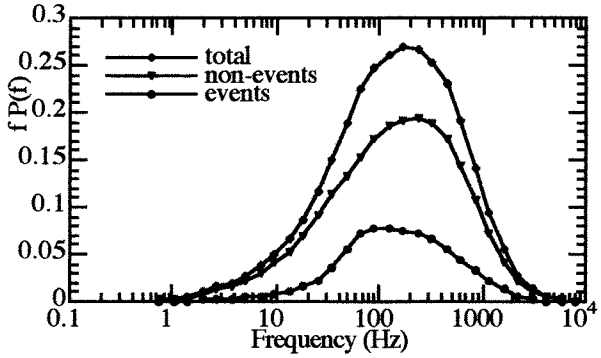

FIGURE 14 - Mean and conditional wavelet velocity spectra at $y^+ = 15$

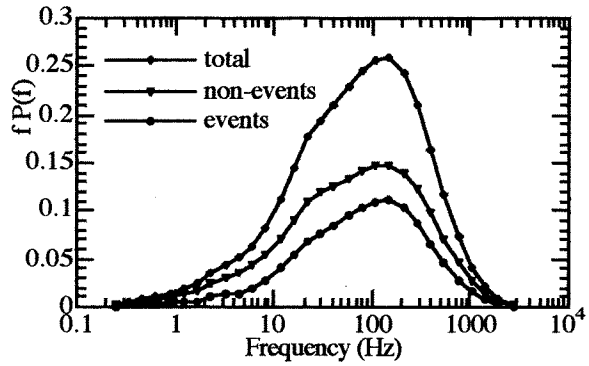

FIGURE 15 - Mean and conditional wavelet temperature spectra at $y^+ = 15$

The conditional spectra for the event instants and for the non event instants are shown. All diagrams are normalised with respect to the total energy of the signals. The spectra for the non event part of the signal have been obtained masking the wavelet energy map with the function [1-DW(f,τ)], before integrating respect to the time. The conditional spectra for the events have been obtained by difference between the total spectra and the non event spectra. Apart from the energetic content of the diagrams,

the spectral distributions appear to be not very dissimilar for the mean spectrum and for the conditional one. A tendency to a slight shift towards the small scales is observed for the event energy distribution respect to the mean distribution. This is in agreement with the results in figure 13.

In figures 14 and 15 detected burst motions contains about 30% of the total energy, both for the velocity and temperature signals.

Conclusions

Analysis of hot wire measurements of the velocity and temperature in a thermal boundary layer have been shown in comparison with published data.

A contribution to the study on the identification of the characteristic turbulent events have been given applying continuous wavelet transform to data measured at a distance of $y^+ = 15$ from the wall, where high turbulent activity is expected.

Results obtained, detecting events by tresholding the wavelet energy map for the velocity and the temperature signals, have been used to determine the distribution of events between scales and to show conditional event spectra in comparison to mean spectra. It has been shown that, even if well defined peak values are present, a large range of scales (frequencies) is involved in the considered characteristic turbulent events.

The velocity and temperature signals lead to very similar results, showing that the temperature may be used, as a passive scalar marker for event detection, at least when the wall temperature is only slightly different from the temperature of the external flow, as in the present case.

The results here obtained are consistent with the scenario supported by recent results coming from the direct numerical simulation. From these studies [4,17], it may be deduced that the turbulent intermittent activity detected by hot wire is produced by the passage of quasi-streamwise vortices at different distance from the measurement points, with different orientation, strength and convective velocity, rather than by localised temporary intermittent eruptions of fluid from the wall or violent inrush of external fluid into the wall region

Acknowledgements

The authors are grateful to Mr Alessandro Mortellaro for the great help given in collecting the data. This research is in part sponsored by the M.U.R.S.T. and in part by the C.N.R..

References

[1] Kline, S.J., Reynolds, W.C., Schramb, F.A., Runstadler, P., "The structure of turbulent boundary layers", *Journal of Fluid Mechanics*, 30, 741 (1967)

[2] Corino, E.R., Brodkey, R.S., "A visual investigation of the wall region in turbulent flow", *Journal of Fluid Mechanics*, 37, 1 (1969)

[3] Hussain, A.K.M.F., "Coherent structures and turbulence", *Journal of Fluid Mechanics*, 173, 303 (1986)

[4] Robinson, S.K., "Coherent motion in the turbulent boundary layer", *Annual Rev. Fluid. Mech.*, 23, 601 (1991)

[5] Lu, S.S., Willmarth, W.W., "Measurement of structure of the Reynolds stress in a turbulent boundary layer", *Journal of Fluid Mechanics*, 60, 481 (1973)

[6] Blackwelder, R.F., Kaplan, R.E., "On the bursting phenomenon near the wall in boundary layer turbulent shear flows", *Journal of Fluid Mechanics*, 76, 89 (1976)

[7] Blackwelder, R.F., Haritonidis, J.H., "Scaling of bursting frequency in turbulent boundary layers", *Journal of Fluid Mechanics*, 132, 87 (1983)

[8] Bogard, D.G., Tiederman, W.G., "Burst detection with single-point velocity measurements", *Journal of Fluid Mechanics*, 162, 389 (1986)

[9] Luchik, T.S., Tiederman, W.G., "Time scale and structure of ejections and burst in turbulent channel flows", *Journal of Fluid Mechanics*, 174, 529 (1987)

[10] Morrison, J.F., Tsai, H.M., Bradshaw, P., "Conditional-sampling schemes for turbulent flow, based on the variable-interval-time-averaging algorithm", *Exp. in Fluids* 7, 173 (1989)

[11] Lu, L.J., Smith, C.R. "Use of flow visualization data to examine spatial-temporal velocity and burst-type characteristics in a turbulent boundary layer", *Journal of Fluid Mechanics*, 232, 303 (1991)

[12] Morrison, J.F., Subramanian, C.S., Bredshaw, P., "Burst and low of the wall in turbulent boundary layers", *Journal of Fluid Mechanics*, 241, 75 (1992)

[13] Wietrzak, A., Lueptow, R.M., "Wall shear stress and velocity in a turbulent axisymmetric boundary layer", *Journal of Fluid Mechanics*, 259, 191 (1994)

[14] Kim, J., Moin, P., Moser, R. "Turbulence statistics in fully developed channel flow at low Reynolds number", *Journal of Fluid Mechanics*, 177 (1987)

[15] Bernard, P.S., Handler, R.A., "Reynolds stress and physics of turbulent momentum transport", *Journal of Fluid Mechanics*, 220, 99 (1990)

[16] Johanssen, A.V., Alfredsson, P.H., Kim, J., "Evolution and dynamics of shear-layer structures in near-wall turbulence", *Journal of Fluid Mechanics*, 224, 579 (1991)

[17] Bernard, P.S., Thomas, J.M., Handler, R.A., "Vortex dynamics and production of Reynolds stress", *Journal of Fluid Mechanics*, 253, 385 (1993)

[18] Brooke, J.W., Hanratly, T.J. "Origin of turbulence producing eddies in a channel flow", *Phys. of Fluids A* 5, (4), 1011 (1993)

[19] Antonia, R.A., Browne, L.W.B., Fulachier, L. "Spectra of velocity and temperature fluctuations in the intermittent region of a turbulent wake " *Phys.-Chem. Hydrodynamics* 8, (2), (1987)

[20] Chen, C., Blackwelder, R.F., "The large motion in a turbulent boundary layer: a study using temperatue contamination", *Journal of Fluid Mechanics*, 89, 1 (1978)

[21] Kim, J., Moin, P., "Transport of passive scalars in a turbulent channel flow" *Turbulent shear flows 6*, Springer-Verlag (1989)

[22] Antonia, R.A., Fulachier, L., Krishnamoorthy, L.V.,

Benabid, T., Anselmet, F., "Influence of wall suction on the organized motion in a turbulent boundary layer", *Journal of Fluid Mechanics*, 190, 217 (1988)
[23] Antonia, R.A., Fulachier, L., "Topology of a turbulent boundary layer with and without wall suction", *Journal of Fluid Mechanics*, 198, 429 (1989)
[24] Benaissa, A., Liandrat, J., Anselmet, F., "Spectral contribution of coherent motions in a turbulent boundary layer", *Eur. J. Mech., B/Fluids*, 14, 697, (1995)
[25] Nagano, Y., Tagawa, M. "Coherent motions and heat transfer in a wall turbulent shear flow", *Journal of Fluid Mechanics*, 305, 127 (1995)
[26] Alfredsson, P.H., Johansson, A.V., "Time scales in turbulent channel flow", *Phys. of Fluids.*, 27, 1974, (1984)
[27] Johansson, A.V., Alfredsson, P.H., "On the structure of a turbulent channel flow", *Journal of Fluid Mechanics*, 122, 295 (1982)
[28] Farge, M., "Wavelet transforms and their applications to turbulence", *Annu. Rev. Fluid. Mech.* 24, 395 (1992)
[29] Liandrat, J., Moret-Bailly, F., "The wavelet transform: some applications to fluid dynamics and turbulence", *Eur. J. Mech. B/Fluids* 9, 1 (1990)
[30] Daubechies, I. *Ten Lectures on Wavelets*, SIAM, Philadelphia, (1992)
[31] Chui, C. *An Introduction to Wavelets* Academic Press, New York, (1992)
[32] Hudgins, L., Friehe, C.,A., Mayer, M.,E., "Wavelet Transforms and Atmospheric Turbulence", *Phys. Rev. Lett.* 71, (20), 3279 (1993)
[33] Erm, L.P., Joubert, P., "Low Reynolds number in a turbulent boundary layer", *Journal of Fluid Mechanics*, 230, 1 (1991)
[34] Lewalle, J. , "Wavelet transforms of some equations of fluid mechanics", *Acta Mech.* 104, 1 (1994)
[35] Higuchi, H., Lewalle, J., Crane, P., "On the Structure of a Two-Dimensional Wake behind a Pair of Flat Plates", *Phys. of Fluids.*, 6, 297, (1994)